Geochimica et Cosmochimica Acta, Vol. 69, No. 9, pp. 2419–2430, 2005
Copyright © 2005 Elsevier Ltd
Printed in the USA. All rights reserved
0016-7037/05 $30.00 + .00

doi:10.1016/j.gca.2004.09.016

Low-pressure adsorption of Ar, Kr, and Xe on carbonaceous materials (kerogen and carbon blacks), ferrihydrite, and montmorillonite: Implications for the trapping of noble gases onto meteoritic matter

Yves Marrocchi,[1,*,†] Angelina Razafitianamaharavo,[2] Laurent J. Michot,[2] and Bernard Marty[1,3]

[1]Centre de Recherches Pétrographiques et Géochimiques, CNRS UPR 2300, 15 rue Notre-Dame des Pauvres, BP20, 54501 Vandoeuvre lès Nancy Cedex, France

[2]Laboratoire Environnement et Minéralurgie, 54501 Vandoeuvre lès Nancy Cedex, France

[3]Ecole Nationale Supérieure de Géologie, Rue du Doyen Roubault, BP 40, 54501 Vandoeuvre lès Nancy Cedex, France

(*Received March* 10, 2004; *accepted in revised form September* 13, 2004)

Abstract—Noble gases trapped in meteorites are tightly bound in a carbonaceous carrier labeled "phase Q." Mechanisms having led to their retention in this phase or in its precursors are poorly understood. To test physical adsorption as a way of retaining noble gases into precursors of meteoritic materials, we have performed adsorption experiments for Ar, Kr, and Xe at low pressures (10^{-4} mbar to 500 mbar) encompassing pressures proposed for the evolving solar nebula. Low-pressure adsorption isotherms were obtained for ferrihydrite and montmorillonite, both phases being present in Orgueil (CI), for terrestrial type III kerogen, the best chemical analog of phase Q studied so far, and for carbon blacks, which are present in phase Q and can be considered as possible precursors.

Based on adsorption data obtained at low pressures relevant to the protosolar nebula, we propose that the amount of noble gases that can be adsorbed onto primitive materials is much higher than previously inferred from experiments carried out at higher pressures. The adsorption capacity increases from kerogen, carbon blacks, montmorillonite to ferrihydrite. Because of its low specific surface area, kerogen can hardly account for the noble gas inventory of Q. Carbon blacks in the temperature range 75 K–100 K can adsorb up to two orders of magnitude more noble gases than those found in Q. Irreversible trapping of a few percent of noble gases adsorbed on such materials could represent a viable process for incorporating noble gases in phase Q precursors. This temperature range cannot be ruled out for the zone of accretion of the meteorite precursors according to recent astrophysical models and observations, although it is near the lower end of the temperatures proposed for the evolving solar nebula. *Copyright © 2005 Elsevier Ltd*

1. INTRODUCTION

Extraterrestrial noble gases trapped in primitive meteorites are important tracers for understanding the history of the early solar system. Although noble gases trapped in primitive meteorites are present in different carriers (e.g., graphite, diamonds, SiC; Lewis et al., 1987; Anders and Zinner, 1993; Zinner, 1998; Nittler, 2003), the main noble gas carrier, also referred to as "phase-Q" or "P1" (hereafter labeled phase Q), is closely associated with carbonaceous material (Lewis et al., 1975; Ott et al., 1981). The nature of the residue obtained after demineralization of bulk samples by HF and HCl which contains phase Q is poorly characterized. It appears to be composed mainly of aromatic moieties linked by short aliphatic chains for which the best chemical terrestrial analog is type III kerogen (Gardinier et al., 2000; Remusat et al., 2003).

Trapped noble gases in chondrites share common characteristics. First, they are concentrated in the carbonaceous residue obtained after acid attack of chondrites, which accounts for a very small fraction (≈1%) of the total mass of the meteorite. Second, noble gases are tightly bound and have high release temperatures under vacuum of up to 1000°C, which suggests that they are associated with retentive sites (Busemann et al., 2000). Third, these gases are released upon oxidation using HNO_3. Fourth, the noble gas elemental abundance patterns are strongly fractionated by up to six orders of magnitude relative to Solar, with marked depletions of light relative to heavy noble gases.

Q-noble gases from different types of primitive meteorites exhibit comparable elemental and isotopic compositions (Wieler et al., 1991, 1992; Huss et al., 1996; Busemann et al., 2000; Busemann and Eugster, 2002). These similarities suggest that one single reservoir, homogeneously mixed and distributed, existed before or during the accretion of planetary bodies. Thus, a common process could have determined the characteristics of Q noble gases in the asteroid region of the solar system (Ozima et al., 1998; Pepin, 2003) or in the protosolar molecular cloud (Huss and Alexander, 1987). Mechanisms leading to the trapping of noble gases in carbonaceous carriers are poorly understood. In the case of xenon, active capture, or "anomalous adsorption," was shown to occur on freshly crushed mineral surfaces in ultra-high vacuum conditions (Bernatowicz et al., 1982; Garrison et al., 1987). In the presence of ionizing radiations, Kr and Xe were also shown to exhibit active capture in silicate smokes (Nichols et al., 1992) and in growing low-Z metal films (Hohenberg et al., 2002). According to Hohenberg et al. (2002), anomalous adsorption may account for the large noble gas concentration of phase Q. Another hypothesis put forward to explain this high concentration is trapping during

* Author to whom correspondence should be addressed (yvesm@crpg.cnrs-nancy.fr).

† *Present address:* McDonnell Center for Space Sciences, Laboratory of Physics, Washington University, St. Louis, Missouri, 63130 USA

condensation of gaseous carbonaceous materials (Frick, 1979; Niemeyer and Marti, 1981; Suzuki and Matsuda, 1990). Gas adsorption could also represent one of the mechanisms leading to noble gas trapping in phase Q precursors, thus accounting for the relative enrichment of heavy noble gases. On the basis of high-resolution transmission electron microscopy studies, Vis et al. (2002) proposed recently that the most plausible process leading to noble gas trapping could be low-temperature adsorption on concave carbonaceous surfaces.

Previous adsorption experiments succeeded in reproducing Q-like elemental abundance patterns (Fanale and Cannon, 1972; Niemeyer and Marti, 1981; Yang and Anders, 1982a,b; Wacker, 1989). However, extrapolated to plausible nebular pressures, the adsorbed noble gas amounts computed from these results were lower than those of phase Q by about four orders of magnitude. It is important to note that these experiments were carried out at pressures (for example $\approx 5\ 10^{-4}$ mbar for Xe; Wacker et al., 1985) not relevant to those inferred for the evolving solar nebula (hereafter SN; $\approx 10^{-13}$ to 10^{-14} mbar for Xe; Ozima and Podosek, 2002). This could have led to erroneous conclusions on the role of adsorption (Yang and Anders, 1982a,b; Wacker et al., 1985).

Noble gas adsorption is a reversible surface process that does not involve trapping in the structure of organic matter. However, it has been shown that noble gases were retained after months of exposure to vacuum and that ~1–10% could be trapped (Niederman and Eugster, 1992), and only released upon oxidation (Yang et al., 1982; Zadnik et al., 1985). In addition, terrestrial noble gas contamination in Allende samples was found to be released at temperatures between 700 to 1000 °C, suggesting that noble gas adsorbed at low temperature could be tightly bound (Srinivasan et al., 1978). It must be pointed out that terrestrial weathering may also play a role in trapping (Scherer et al., 1996).

To document adsorption at low pressure relevant to the early evolution of the solar nebula (Wood and Morfill, 1988; Cassen, 1994; Cameron, 1995; Dubrulle et al., 1995; Bell, 1999), we report results of experiments designed to study the adsorption of Ar, Kr, and Xe at very low pressure. In addition, such experiments allow one to probe the most energetic surface sites of the materials investigated, i.e., the surface sites that are most likely relevant in noble gas trapping. Low-pressure adsorption isotherms were obtained on terrestrial type III kerogen (considered to be the best chemical analog of phase Q studied so far; Gardinier et al., 2000), carbon blacks (considered as a possible precursors of meteoritic organic matter; hereafter CB; Zadnik et al., 1985; Vis et al., 2002) subjected to various physical and/or chemical treatments, and two mineral phases known to be present in primitive extraterrestrial material (e.g., Orgueil) and having contrasted surface chemistry and area, ferrihydrite, and montmorillonite.

2. MATERIALS AND METHODS

2.1. Samples

Ferrihydrite. Ferrihydrite was synthesized according to procedures described in Cornell and Schwertmann (1996) and Liang et al. (2000). A solution of 0.05M $Fe(NO_3)_3$ was rapidly titrated to a pH of ~10 by dropwise addition of 0.1M KOH. The resulting precipitate was dialyzed to remove excess salts and finally dried at 50°C in air. X-ray diffraction and Mossbauer analyses were performed to confirm that the synthesized sample was two-line ferrihydrite.

Montmorillonite. The montmorillonite used in this study is a sample from Wyoming (Swy2) purchased from the Source Clays Repository at Purdue University, Indiana, USA. Before use, it was sodium-saturated by exchanging it three times in a 1M NaCl solution. The resulting slurry was washed extensively by centrifugation and redispersion in MilliQ water. After each centrifugation, the bottom of the centrifuge tube that contained various impurities such as quartz, feldspar, and iron oxide was discarded. The purity of the final air-dried sample was checked by X-ray diffraction.

Kerogen. It has been suggested that terrestrial kerogen represents a relevant chemical analog of Q (Gardinier et al., 2000). We used type III kerogen (Dogie Creek, Wyoming, USA), whose chemical composition is close to that of Q in primitive carbonaceous chondrites such as Orgueil and Murchinson (Table 1).

Table 1. Chemical composition of meteoritic insoluble organic fraction and kerogen used in this study. The chemical composition was normalized to 100 carbon atoms (Gardinier et al., 2000).

	Composition[a]
Orgueil (CI)	$C_{100}H_{72}O_{10}N_2S_4$
Murchinson (CM)	$C_{100}H_{71}O_{12}N_3S_2$
Allende (CV)[b]	$C_{100}H_{1.8}O_?N_{0.5}S_4$
Tagish Lake (C?)	$C_{100}H_{46}O_{15}N_{10}S_?$
Kerogen type III[c]	$C_{100}\ H_{75}\ O_{9.2}N_2$

[a] Chemical composition normalized at 100 carbon atoms.
[b] Strong alteration induced by metamorphism (CV6).
[c] Less mature type III kerogen.

Carbon blacks. Even if kerogen is chemically close to the insoluble organic fraction of meteorites, it probably has significant structural differences with Q. In addition, recent combustion experiments (Verchovsky et al., 2002) strongly suggest that only minor combustible constituents of the macromolecular organic matter of meteorites are the noble gas carriers. This phase is probably the result of maturation of different precursors. Organic matter in the interstellar medium (ISM) is formed of simple molecules (<100 amu), whereas meteoritic organic matter presents macromolecular structures composed of aromatic moieties linked by short aliphatic chains (Robert, 2002). In view of this uncertainty, it is relevant to test various carbonaceous materials for their adsorption capacity to assess the influence of adsorption energy and specific surface area. Recent high-resolution transmission electron microscopy observations of organic material in the Allende (CV3), Leoville (CV3), and Vigarano (CV3) meteorites have revealed the presence of abundant carbon-black particles that are not observed in type III kerogen (Vis et al., 2002). Low-pressure argon adsorption experiments were carried out on carbon blacks subjected to various physical or chemical treatments. We used carbon black MT 990 (medium particles, thermal black) from HUBER Corp. Four sets of samples were prepared using physical or chemical treatments. The first set of CB was oxidized by H_2O_2 at 95°C for 6 h using the protocol defined by Sosa et al. (1993). A second set of CB (50 $g.L^{-1}$) was attacked by HNO_3 10M at 95°C for 6 h. The suspension was centrifuged and carbon washed by resuspension with water, shaken for 4 h, centrifuged and dried at 90°C for 12 h in a vacuum chamber at less than 1500 Pa. Another CB aliquot was oxidized with oxygen at 600°C for 1 h and cooled in a flow of He (Sosa et al., 1996). Graphitized CB was obtained by treatment of the MT 990 at 2700°C for 48 h, followed by cooling in an inert atmosphere.

2.2. Experimental Procedure

Two types of gas adsorption setups were used in this study. (i) The first experiment, based on the classical Brunauer Emmet Teller method (hereafter BET, Brunauer et al., 1938), allowed us to determine the adsorption capacity of the adsorbent (namely the volume of the mono-

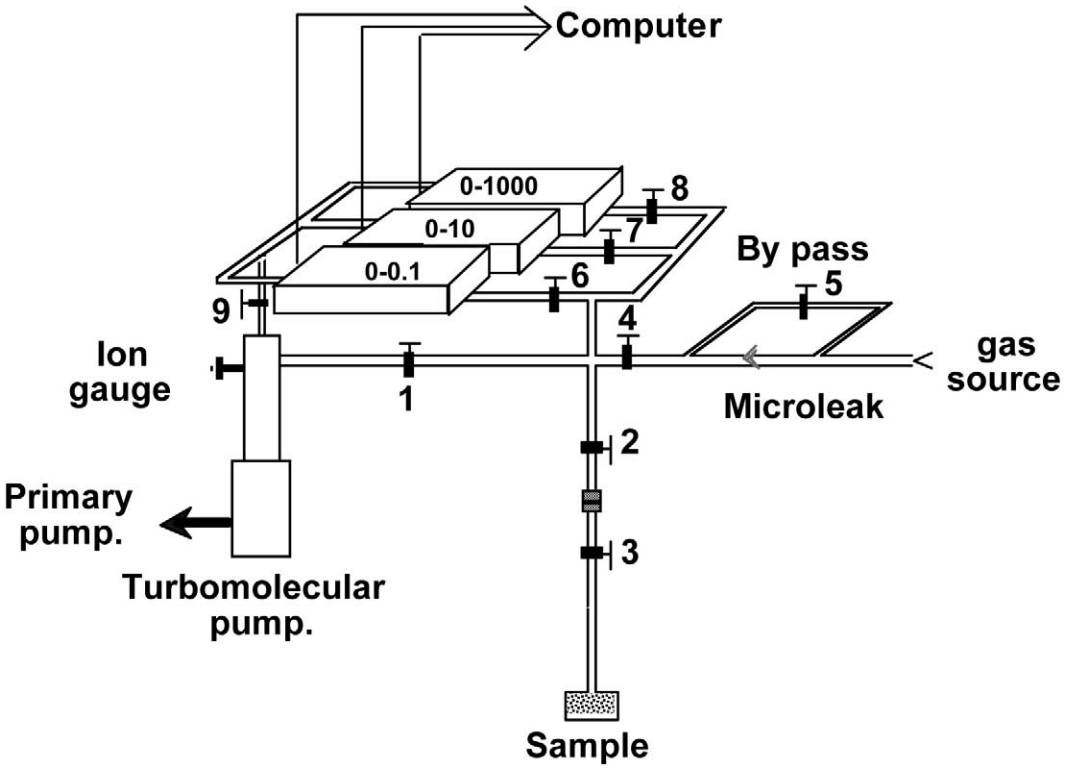

Fig. 1. Scheme of the quasi-equilibrium adsorption volumetry apparatus. The pressure range of the three high-precision pressure gauges is in mbar. Tube diameters are 8 mm.

layer for each studied material). (ii) The second experiment was designed to measure adsorption parameters of noble gases at very low pressure.

(i) The first experimental setup is a step-by-step volumetric adsorption device. In such a setup, adsorbate gaseous molecules are first introduced in a known volume kept at 298 K. The pressure is recorded and the adsorbate is then put into contact with the adsorbent (sample) kept at a constant temperature (in the case of nitrogen, 77 K, corresponding to a saturating vapor pressure of 1.01 bar). The pressure drops and stabilizes towards a value called the equilibrium pressure. The amount of molecules adsorbed at equilibrium pressure is computed from the equilibrium pressure and the volumes of the line which had been previously calibrated using helium. The adsorbate pressure is then increased by a given increment until a new equilibrium pressure is reached. The procedure is repeated step by step, allowing the adsorption isotherm of the adsorbent to be established. Stepwise desorption is carried out in a similar way, to characterize the microstructure of the adsorbent. Indeed, the desorption isotherm differs from the adsorption isotherm depending on the nature of pores and their size distribution (Gregg and Sing, 1982).

Approximately 500 mg of sample were outgassed overnight at 298 K (kerogen, CBs), 323 K (ferrihydrite), and 383 K (montmorillonite). The specific surface areas were then determined using the classical BET method (Brunauer et al., 1938), and the presence of micropores (diameter lower than 2 nm) was assessed using the *t*-plot method (De Boer et al., 1966). According to the BET theory, the isothermal adsorption of vapor on a solid surface can be described by the following equation:

$$\frac{P/P_0}{V(1-P/P_0)} = \frac{1}{V_m C} + \left(\frac{C-1}{V_m C}\right)\left(\frac{P}{P_0}\right) \quad (1)$$

where V is the volume of adsorbate per gram of adsorbent (in cm^3 $STP.g^{-1}$) at equilibrium pressure P, P_0 is the saturating vapor pressure, V_m is the volume of gas equivalent to a single monolayer, and $C = \exp[(E_1 - E_L)/RT]$ where E_1 is the adsorption energy of the first layer of adsorbed gas on the solid and E_L the energy of liquefaction of the adsorbate (Brunauer et al., 1938). In the relative pressure range (P/P_0) between 0.05 and 0.25, this equation is generally valid, which allows the determination of both V_m and C. Indeed, in a plot of $y = (P/P_0)/V(1 - P/P_0)$ as a function of $x = P/P_0$, Eqn. 1 yields a straight line whose slope and intercept are $(C - 1)/V_mC$ and $1/V_mC$, respectively. V_m can be converted into a specific surface area value using the cross sectional area of the adsorbate (in the case of N_2, $\sigma_m = 16.26$ Å^2; McClellan and Harnsberger, 1967).

(ii) The second experiment is a quasi-equilibrium gas adsorption device developed in LEM (Laboratoire Environnement et Minéralurgie), Nancy. It is difficult to get isotherm data at very low pressures following the step-by-step equilibrium method outlined above, because the time required to reach equilibrium can be exceedingly long and because the resolution of measurements is poor in this low-pressure range (Michot et al., 1990). To circumvent this problem, a quasi-equilibrium method has been developed in which the adsorbate is introduced in the cell through a calibrated microleak at a flow rate sufficiently slow (≈0.05 $cm^3.min^{-1}$) to ensure equilibrium all along the adsorption isotherm (Fig. 1; Michot et al., 1990, 1998; Villiéras et al., 1992, 1996, 1997, 1999; Michot and Villiéras, 2002). The gas flow in the system is controlled by the pressure in the volume adjacent to the microleak. The first phase of the experiment is to measure the pressure evolution in the system as a function of time without adsorbent. To do so, the pumping system and the volume in which the adsorbent is loaded are isolated (valves 1 and 2 closed, Fig. 1). The evolution of pressure vs. time is linear, therefore the adsorption on the internal walls of the line is negligible. The system is then pumped down (valve 4 closed and valves 1 and 2 open) to a pressure of 10^{-6} mbar (measured with an ion gauge located close to the pump, Fig. 1). After stabilization of the vacuum, the pressure gauges that will be used for measuring noble gas pressures (see below) are reset to zero. These pressure gauges admit a detection limit of 10^{-4} mbar, giving an upper limit for the static vacuum during the experiments. A separate experiment checked that

the gauges remained at zero in static condition (i.e., pumps closed), for the duration typical of the adsorption experiments, indicating that the static pressures were always lower than 10^{-4} mbar.

The same experiment is repeated but this time in the presence of the adsorbent (valve 2 open, Fig. 1). Knowing the volume of the system, the flow rate, and taking into account both the non-ideality of the adsorbate and thermal effusion corrections that are crucial for measurements at low pressure, the amount of adsorbed gas is calculated by comparing the resulting evolution curves obtained with, and without, adsorbent (Villiéras et al., 1996). The experimental device is equipped with three high-precision capacitance manometers (0–0.1 mbar, 0–10 mbar, 0–1000 mbar, Baratron) allowing measurement of pressures in the range 10^{-4} mbar to 500 mbar. The measured pressures (P) are then divided by the saturating vapor pressures (P_0) at the temperature of the adsorbent. Because the temperature of the latter differs from that of the pressures gauges, a correction for thermal transpiration is applied (Takaishi and Sensui, 1963). This correction allows one to compute the pressure of a gas in a cold region from the pressure measured in a warmer region (Dusham and Lafferty, 1962). This is the case of our experiment because the pressure gauge is at room temperature, whereas the gas in contact with the adsorbate is at liquid nitrogen temperature. Correction for thermal transpiration, computed for example using equation and coefficients given in Takaishi and Sensui (1963), can reach several orders of magnitude (Podosek et al., 1981). At 77 K, the Ar and Kr saturating vapor pressures are 0.18 bar and 1.32 10^{-3} bar, respectively. In this study, the relative pressures (P/P_0) were in the range $10^{-8}$to 0.15 for Ar and Kr. At 77 K, the xenon vapor pressure is very low (1.17 10^{-6} bar), prohibiting a precise measurement of the Xe pressure with our experimental setup. For this reason, the xenon adsorption experiments were carried out at 196 K. At this temperature, the Xe saturating vapor pressure is 4.78 bar, which allows us to investigate pressures in the range 10^{-10}–0.1, taking into account the correction for thermal transpiration (Takaishi and Sensui, 1963).

Approximately 1 g of sample was used for each experiment. Before adsorption, the samples were outgassed overnight at 298 K (kerogen, CBs), 323 K (ferrihydrite), and 383 K (montmorillonite) until a residual pressure of 10^{-6} mbar was reached. The frequency of measurements was adjusted to get ~200 experimental points per unit of ln (P/P_0), and the duration of a complete measurement was approximately 15 h. This method allowed us to obtain information on the initial stages of adsorption and to determine the adsorption parameters at pressures that are close to those estimated for the solar nebula (Fig. 2). Between 2000 and 3000 data points could be collected for relative pressures (P/P_0) < 0.15.

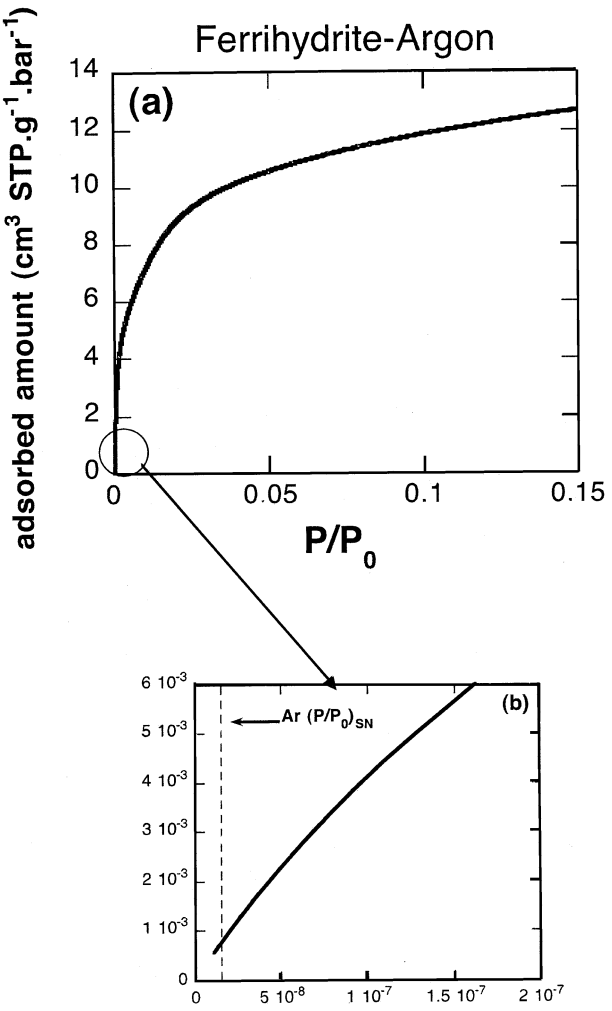

Fig. 2. (a) Argon adsorption isotherm on ferrihydrite at 77 K. (b) Expanded view of (a) towards the low-pressure range of the argon adsorption isotherm. Experimental setup allowed accurate measurements in the very low pressure range, from 10^{-4} mbar to 500 mbar, corresponding to relating pressures of 10^{-8} to 0.15 for argon and krypton, and 10^{-10} to 0.1 for xenon (see text for thermal transpiration correction). The isotherm covers the argon partial pressure range typical of the solar nebula. Kr and Xe adsorption isotherms do not cover the SN partial pressure range but Henry's law behavior is expected at very low pressure. Adsorption constants were determined using the very low pressure adsorption isotherm.

3. RESULTS

3.1. Nitrogen Adsorption

Nitrogen adsorption-desorption isotherms were determined to yield specific surface area and pore size distribution for each of the samples. Although this information is not directly relevant to the study of noble gas adsorption, it provides general information about the adsorption behavior of the samples that can be helpful in the interpretation of low-pressure data, especially regarding the potential importance of micropores. For kerogen, the shape of the adsorption-desorption isotherm of nitrogen (Fig. 3a) reveals a weak affinity between the adsorbate and the adsorbent as the amount adsorbed does not increase strongly at low P/P_0 (Gregg and Sing, 1982). In this case, the use of the BET equation for determining the surface area is questionable as monolayer completion is not really distinguishable from multilayer formation. Still, we decided to apply such a procedure to obtain at least some estimate of the "surface area" of kerogen. The value thus obtained is rather low, approximately 4 m^2/g (Table 2). The adsorption-desorption isotherm of nitrogen on ferrihydrite (Fig. 3b) is typical of a solid presenting a quasi-continuous distribution of pore sizes in the transition range between large micropores and small mesopores and with a small external surface area (Hofmann et al., 2004). The total specific surface area derived from the BET treatment is high, approximately 400 m^2/g (Table 2). The nitrogen adsorption-desorption isotherm on montmorillonite (Fig. 3c) reveals the presence of both micropores and mesopores and a specific surface area around 80 m^2/g. The t-plot treatment (De Boer et al., 1966) yields a nonmicroporous surface area of 50 m^2/g and an equivalent microporous surface area of approximately 30 m^2/g (Table 2). CB samples are characterized by the absence of micropores and present specific surface area in the range 5.5–11.6 m^2/g,

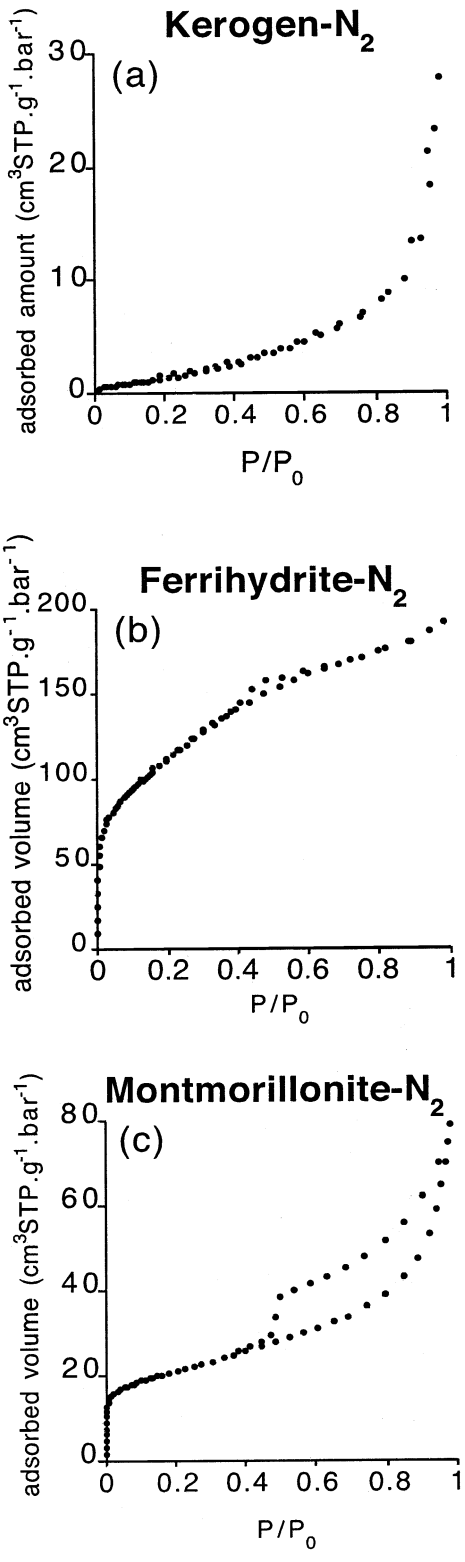

Fig. 3. (a) Nitrogen adsorption isotherm on kerogen at 77 K. (b) Nitrogen adsorption isotherm on ferrihydrite at 77 K. (c) Nitrogen adsorption isotherm on montmorillonite at 77 K. Specific surface areas were determined using these isotherms and the BET equation (Brunauer et al., 1938).

depending on the nature of the applied chemical or physical treatments (Table 3).

3.2. Noble Gas Adsorption

Heterogeneous surface domains with different adsorption potentials are present in all natural samples. To each domain corresponds a specific adsorption behavior, yielding different values for the Henry's coefficient (Fig. 2). As a result, the relationship between adsorbed amount and pressure is not linear, so that Henry's law is only an approximation that can be applied in a given range of pressure. Previously, most adsorption experiments were carried out at relatively high pressures, in adsorption domains corresponding to low slopes of the adsorbed amount vs. pressure correlations, thus yielding low Henry's coefficients (Fanale and Cannon, 1972; Niemeyer and Marti, 1981; Yang and Anders, 1982a,b; Wacker, 1989). Extrapolation of these Henry's coefficients to very low pressures will underestimate the amount of adsorbed gas. In the low-pressure range relevant to solar nebula conditions, the correlation is also close to linear (Fig. 4) but with a much steeper slope which corresponds to the progressive filling of the most energetic adsorption sites (Fig. 2).

The linear region can be interpreted in terms of Henry's law

$$\theta_{i,j} = H_{i,j} * P_i \tag{2}$$

where θ is the surface coverage defined as V/V_m for a given adsorbate i and a given adsorbent j, P_i is the partial pressure of i, and $H_{i,j}$ is the Henry coefficient of adsorbent j for adsorbate i that can be written as:

$$H_{i,j} = \frac{[kT]^{1/2}}{[2\pi m_i]^{3/2}} \frac{1}{\overline{\nu}_{a,i,j}^3} e^{\varphi^0_{a,i,j}/kT} \tag{3}$$

where k is Boltzmann constant equal to $1.32\ 10^{-21}$ joules (J)/K, $\overline{\nu}_{a,i,j}$ is the average vibrational frequency of the adsorbed molecule i on the adsorbent j, and $\varphi^0_{a,i,j}$ the energy of the normal adsorbate-adsorbent bond. $H_{i,j}$ can be determined from the slope of the low-pressure adsorption isotherm.

$P_{0,i}$, saturating vapor pressure of adsorbate i, can be expressed as:

$$P_{0,i} = \frac{[2\pi m_i]^{3/2}}{[kT]^{1/2}} \nu^3 e^{-\varphi_{0,i}/kT} \tag{4}$$

where φ_0 is the energy of the normal bond in a crystal of the adsorbate and ν the average vibrational frequency of the adsorbate in a crystal of the adsorbate. When plotting $\theta_{i,j}$ as a function of the relative pressure P/P_0, Eqn. 2 becomes:

$$\theta_{i,j} = H'_{i,j} * (P_i/P_{0,i}) \tag{5}$$

with $H'_{i,j} = H_{i,j} * P_{0,i}$. If one assumes that the average vibrational frequency ν_a of the adsorbed molecule is equal to the average vibrational frequency ν of the adsorbate in a crystal of the adsorbate, then Eqn. 5 reduces to:

$$H'_{i,j} = e^{(\varphi_{a,i,j} - \varphi_0)/kT} \tag{6}$$

For each of the adsorbates, the isotherms exhibit a linear relationship at low relative pressure ($P/P_0 \leq 10^{-4}$; Fig. 4) with

Table 2. Specific area and distribution of pores of investigated samples.

	Specific area (m^2/g)	Micropores (8–20 Å)	Mesopores (20–400 Å)
Kerogen	4.5	no	no
Ferrihydrite	400	large	small
Montmorillonite	80	30 m^2/g	50 m^2/g
Original carbon black	6.8	no	small
Carbon black O_2, 600°C, 1 h	5.5	no	small
Carbon black graphitized, 2700°C, 48 h	7.5	no	small
Carbon black oxidized, H_2O_2, 95°C, 6 h	6.1	no	small
Carbon black oxidized, HNO_3, 10M, 95°C, 6 h	11.6	no	small

correlations coefficients higher than 0.98, allowing a reliable determination of the slope ($e^{(\varphi_{a,i,j}-\varphi_0)/kT}$). Taking into account the temperature of the experiment, it then allows a reliable determination of (φ_a-φ_0) (see Tables 3 and 4 for experimental data and Tables E2–E24 presented in the electronic annex for adsorption parameters computed at various temperatures). The values thus obtained are almost constant at approximately 5.10^{-21} J for kerogen and 8.10^{-21} J for montmorillonite. In the case of ferrihydrite, the value obtained for xenon ($1.6.10^{-20}$ J) is significantly higher than those calculated for Ar and Kr ($\approx 1.10^{-20}$ J), which can be assigned to the porous structure of ferrihydrite. Indeed, because of the continuous pore size distribution of this material, the influence of the adsorbate size can be significant. The same tendency can be observed for montmorillonite but to a lesser extent. Carbon blacks present an important variability of the specific surface area and interaction parameter (φ_a-φ_0) (Table 3) depending on chemical or physical treatments.

4. DISCUSSION

All the results reported in the next subsections have been calculated using the canonical pressure of the solar nebula reported in the literature (10^{-3} mbar; e.g., Pepin, 1991; Ozima and Podosek, 2002) and the noble gas relative abundances in the solar nebula presented in the electronic annex (Table A1, Anders and Grevesse, 1989). In the temperature range discussed below (75 K–90 K), Ar and Kr are in the gaseous state. According to the phase diagram, the solid/gas transition of xenon occurs at a temperature of 70 K for a pressure of 10^{-3} mbar. Therefore, for the temperature range of interest, xenon is also essentially in the gaseous state.

Table 3. Specific surface area, argon adsorption constant at 77 K and adsorbate/adsorbent interaction parameter for various kinds of carbon blacks (CB).

Treatment	Specific area ($m^2 \cdot g^{-1}$)	H 77 K	($\varphi_a - \varphi_0$) Joules
Original CB	6.8	7885	$9.5.\ 10^{-21}$
O_2, 600°C, 1 h	5.5	638	$6.8.\ 10^{-21}$
Graphitized, 2700°C, 48 h	7.5	14356	$1.0.\ 10^{-20}$
Oxidized, H_2O_2, 95°C, 6 h	6.1	13077	$1.0.\ 10^{-20}$
Oxidized, HNO_3, 10M, 95°C, 6 h	11.6	58235	$1.1.\ 10^{-20}$

4.1. Adsorption on Kerogen

Using Eqn. 6 and values of the adsorbate-adsorbent interaction parameters (Table 4), the values of H′ can be calculated for any temperature between 75 K and 150 K for Ar and Kr, and between 75 K and 200 K for Xe. The calculated amounts of noble gases adsorbed at the canonical SN pressure can then be compared to those found in phase Q. In the case of kerogen, this comparison shows that adsorption in the range 75 K–90 K fails to account for the amount of Q gases in Orgueil (Fig. 5). On the basis of data displayed in Figure 5, one can estimate that temperatures less than 70 K would be required to reproduce the abundance patterns of Ar and Kr using type III kerogen as a phase Q analog. The relatively high abundance of xenon will be discussed in the next subsection.

4.2. Adsorption on Potential Phase Q Precursors

Low-pressure argon adsorption isotherms obtained at 77 K for kerogen and for five carbon blacks show that kerogen has

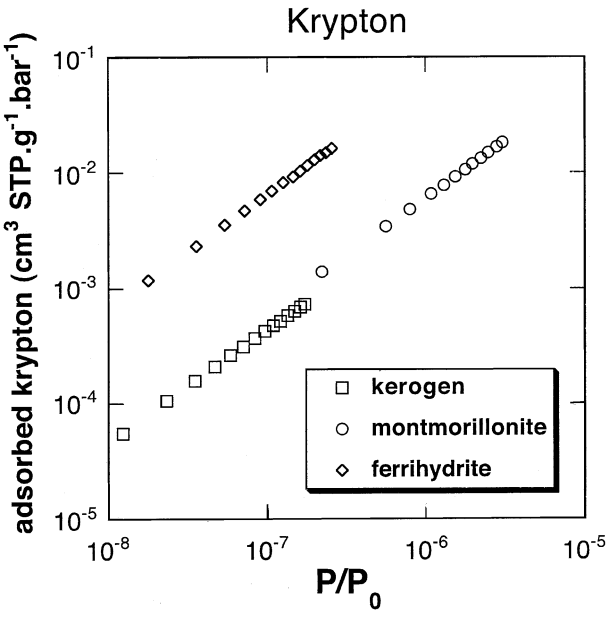

Fig. 4. Argon adsorption isotherm ($P/P_0 \leq 10^{-4}$) for kerogen, montmorillonite, and ferrihydrite at low pressure. The isotherms are linear at low pressure with correlation coefficients >0.98, allowing a reliable determination of the adsorption parameters.

Table 4. Adsorption constant (H′) at experiment temperatures for Ar, Kr, and Xe and resulting adsorbate–adsorbent interaction parameters ($\varphi_a - \varphi_0$).

Sample	Gas	T(K)	H	r^2	$(\varphi_a - \varphi_0)$ Joules
Kerogen	Ar	77	160	0.997	$5.39.10^{-21}$
	Kr	77	158	0.998	$5.38.10^{-21}$
	Xe	196	6.1	0.999	$5.65.10^{-21}$
Ferrihydrite	Ar	77	10950	0.997	$9.88.10^{-21}$
	Kr	77	18800	0.999	$1.04.10^{-20}$
	Xe	196	426	0.994	$1.63.10^{-20}$
Montmorillonite	Ar	77	2000	0.988	$8.07.10^{-21}$
	Kr	77	1570	0.996	$7.82.10^{-21}$
	Xe	196	40	0.998	$9.97.10^{-21}$

the lowest surface area and adsorption energy. Adsorption rates at low pressures, which are a function of surface areas as well as amounts of adsorbed gases, and a function of adsorption energies, are the lowest for kerogen (Fig. 6). As predicted from the shape of the isotherms, the interaction parameters (Table 3) are significantly higher for carbon black samples, the highest value ($1.2\ 10^{-20}$ J) being obtained for the carbon blacks sample oxidized by HNO_3.

On the basis of data obtained for kerogen, montmorillonite, and ferrihydrite (Table 4), it is reasonable to assume that the interaction parameters derived from argon adsorption data can be used for krypton and xenon. Indeed, these three samples present almost the same interaction parameter (φ_a-φ_0) for each of the noble gases investigated. As Kr and Xe adsorption coefficients were not determined for carbon blacks, we extrapolate the Henry's coefficients for Kr and Xe using values of (φ_a-φ_0) determined from the argon isotherm on carbon blacks.

All the carbons blacks investigated present specific surface area and interaction parameters which can reproduce the concentration of Ar and Kr in phase Q of Orgueil at a temperature of 75 K (Fig. 7; the case of xenon is discussed below). In view of the data obtained for carbon blacks subjected to various physical and chemical treatments, a value of $\approx 9.10^{-21}$ J, which is the mean of all carbon blacks investigated in this study, can be taken for (φ_a-φ_0). Taking a surface area value of approximately 10 $m^2.g^{-1}$, which is a value common for carbonaceous materials (Sosa et al., 1996), the computed amount of adsorbed noble gases on carbon blacks can account for the noble gas inventory of carbonaceous matter in primitive meteorites if the temperature is 75 K or lower (Fig. 7). It must be pointed out that the value of 10 $m^2.g^{-1}$ is a minimum considering the very small particle size of carbon blacks observed in phase Q (Vis et al., 2002). Several studies have reported irreversible adsorption of Kr and Xe for some forms of carbonaceous material. Indeed, only 1% to 10% were released at high temperature of 800 to 1000 °C, strongly suggesting trapping in the organic network (Yang et al., 1982; Zadnik et al., 1985). Assuming that only 1% of the originally adsorbed noble gases are irreversibly trapped, the heavy noble gas content of phase Q can be reproduced in the case of adsorption at 75 K on carbon blacks oxidized with HNO_3 (Fig. 8).

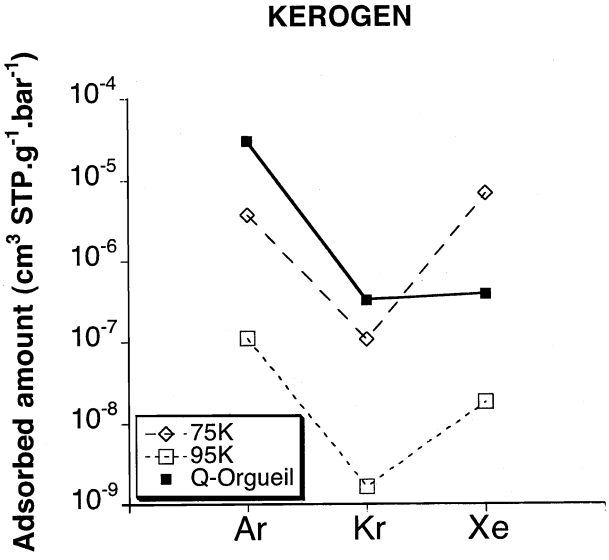

Fig. 5. Elemental fractionation pattern for kerogen at different temperature compared to phase Q pattern of Orgueil (elemental concentration in the acid-resistant meteoritic residues; Huss et al., 1996; Busemann et al., 2000).

As illustrated in Figures 5, 7, and 8, the adsorbed pattern of argon and krypton is comparable to that observed in phase Q, but adsorbed Xe is enriched by two orders of magnitude relative to phase Q. This difference tends to vanish with increasing temperature and within uncertainties for adsorption at 100 K. However, at this temperature the amount of noble gas adsorbed is comparable to that found in phase Q, which leaves little space for irreversible trapping (Fig. 9). We do not have a clear explanation for this Xe overabundance during adsorption relative to phase Q. Part of this discrepancy could be due to the fact that we used a solar noble gas pattern to compute the adsorbed amounts, which may fail to match precisely the original noble gas abundance. For example, xenon is enriched by a factor of 4 in the solar wind relative to the (inferred) solar nebula period (Wieler, 2002).

It is also important to note that here we assume equilibrium adsorption. Considerably higher noble gas amounts could have been trapped if adsorption and phase Q formation took place simultaneously. This view is in agreement with observations of Vis et al. (2002) who reported the presence of onion-like structures with internal voids of ~2 nm where noble gases could be trapped. In a continuous adsorption process taking place at decreasing temperature, it is conceivable that the

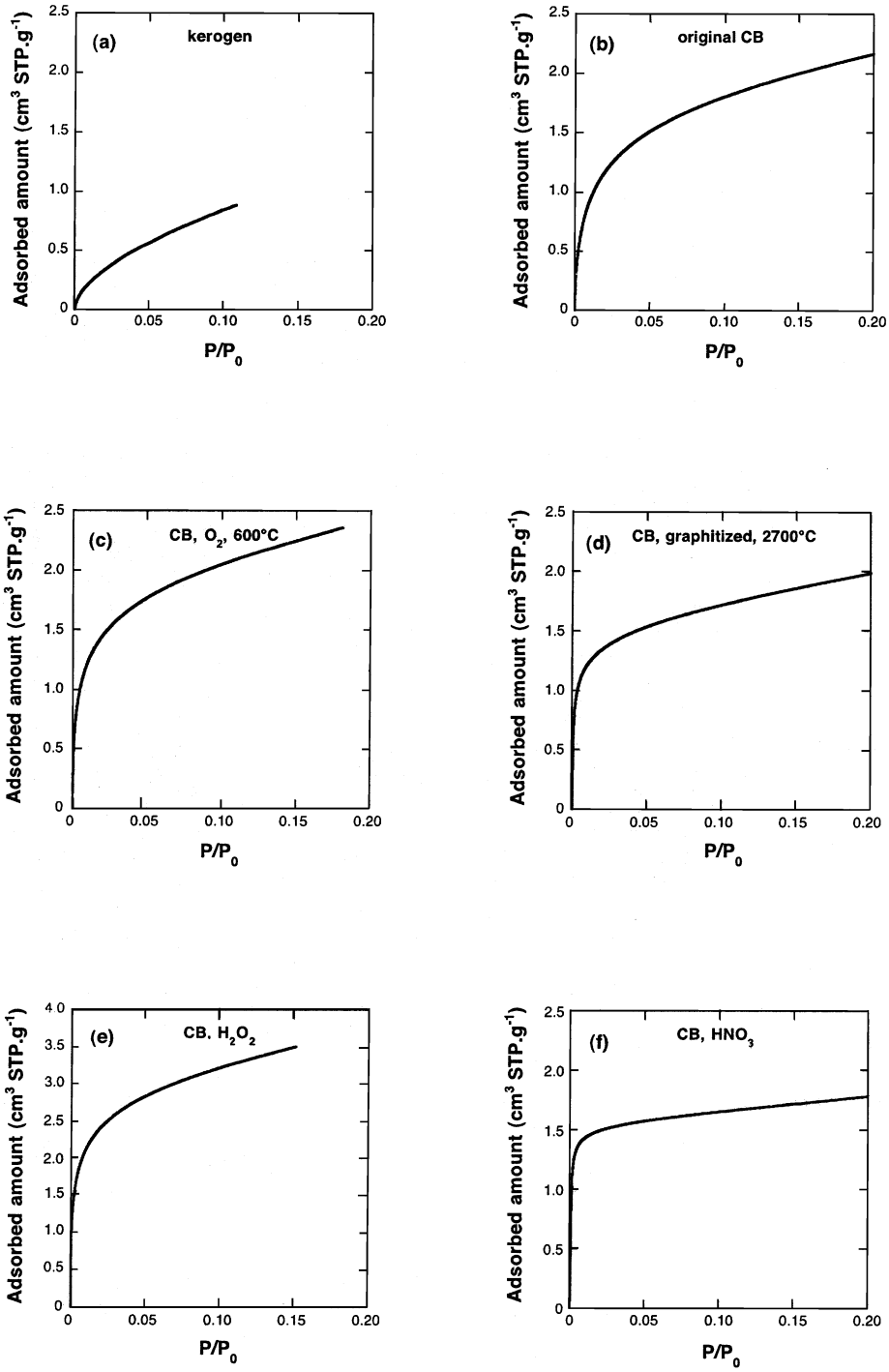

Fig. 6. Low-pressure argon isotherm at 77 K on different materials (a) kerogen, (b) carbon blacks, (c) carbon blacks oxidized at 600°C, (d) carbon blacks graphitized at 2700°C, (e) carbon blacks oxidized with H_2O_2, (f) carbon blacks leached with HNO_3 10M.

amount of trapped noble gases differed for each gas according to the evolution of the partial pressure with temperature.

Although these new experiments show that low-temperature adsorption can account for the amounts of noble gases trapped in Q, they do not provide explanation for the observed isotopic differences between Solar and Q. We are currently investigating isotopic fractionation of noble gas during Rayleigh-like adsorption experiments, but so far we have not detected any measurable isotopic fractionation. If no isotopic fractionation occurs during adsorption, then it is necessary to invoke that noble gases were already fractionated from Solar at the time of adsorption on phase Q. Ozima et al. (1998) have proposed that isotopic and elemental fractionation of solar noble gases occurred during Rayleigh-like gas escape from the solar nebula,

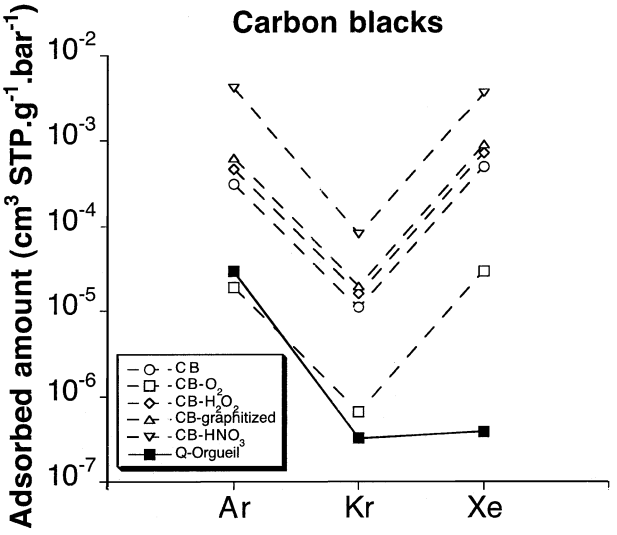

Fig. 7. Elemental fractionation pattern for five carbon blacks at 75 K compared to phase Q pattern of Orgueil.

without specifying the nature of the processes involved. Such a model could account for the isotopic ratios of Q relative to solar fairly well, but discrepancies were observed for elemental ratios, thus leaving open the possibility that further elemental processing was involved. Likewise, Pepin (2003) investigated the possibility that Q fractionation took place either during UV irradiation of the edge of the protosolar disk by a nearby star or during gravitational escape of a methane-rich atmosphere around planetesimals. In both processes, adsorption was invoked as being the major factor in the trapping of noble gases onto grains, although Pepin (2003) acknowledged that there was a problem of quantitative adsorption given adsorption parameters known at that time. The present study, which predicts much higher amounts of adsorbed noble gases onto grains, may revitalize this type of model.

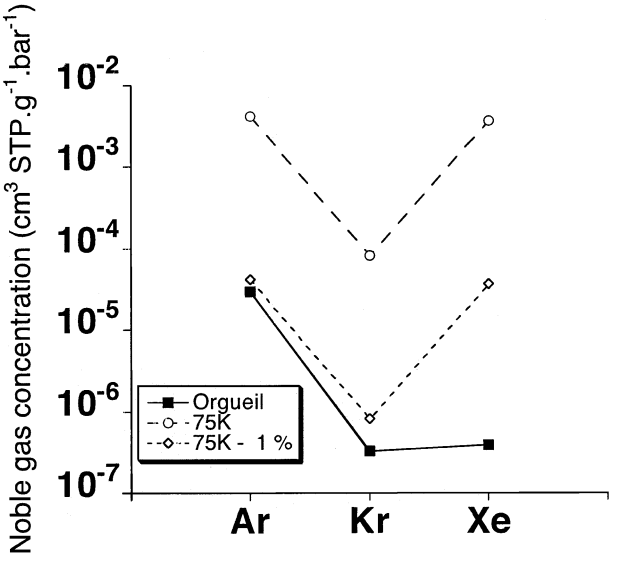

Fig. 8. Elemental fractionation pattern for carbon blacks leached by HNO_3, 10M and 1% adsorbed gas irreversibly trapped compared to phase Q of Orgueil.

4.3. Meteoritic and Astrophysical Constraints on Parent Bodies Accretion

One could argue that the low temperature range needed to account for the noble gas concentration in meteorites is unrealistic. However, the relatively high content of nitrogen in meteoritic organic macromolecules (Table 1) shows that this organic matter has undergone negligible maturation (Ehrenfreund et al., 1991), strongly suggesting that this material has never been heated to temperatures higher than 350 K. This maximum temperature is in good agreement with low temperature processing inferred from our results. In the temperature range of ≈70 K, few species are present, mainly noble gases, H and CO, and one can envision that the synthesis of organic matter occurred concomitantly with noble gas incorporation.

According to some models describing the evolution of the protosolar nebula (Bell et al., 1999) and to recent astrophysical observations (Woolum and Cassen, 1999), temperatures between 60 K and 100 K are currently proposed for the region located between 2 and 3 AU, where accretion of meteorite parent bodies is believed to have taken place. In the standard SN evolution model, the thermal structure is a function of the mass accretion rate ($M_\odot$) corresponding to the mass flow toward the Sun. Higher accretion rates (10^{-5} 10^{-5} $M_\odot$/yr), corresponding to a younger, dustier and more massive disk, would result in a very hot disk, enough to vaporize all but the most refractory materials within few AU of the Sun (Boss, 1993; Bell et al., 1997, 1999; Bell, 1999). It is difficult to precisely estimate the time period over which T-Tauri disks cool from these hot states, but several arguments support the possibility that the mass accretion rate declined drastically in less than 10^5 yr (Humayun and Cassen, 2000). Hartmann et al. (1998) observed 56 class II T-Tauri stars and found that 44 of them have a mass accretion rate between 10^{-7} and 10^{-9} $M_\odot$/yr in the time interval of 3.10^5 to 3.10^6 yr. These models and observations suggest that the hot phase of the solar nebula lasted only for 10^5 years, representing only a short fraction of the solar nebula lifetime. Thus, the mass accretion rate in the SN could have decreased very quickly to reach values (10^{-8} to 10^{-9} $M_\odot$/yr) corresponding to low temperatures in the range 20 K–60 K at 3 AU (Bell, 1999). Despite discrepancies between theoretical estimates of nebula lifetimes (<1 Ma) and timescales constrained by isotopic data for meteorites (several Ma), it seems relevant to consider that meteorite aggregation occurred all along the SN evolution, even at low temperature (Podosek and Cassen, 1994).

Such low temperatures are also required to account for the recent discovery of extrasolar giant planets (hot-Jupiters) located close (less than 0.2 AU) to their central star (Collier Cameron, 2002). The occurrence of planets close to their star suggests that the circumstellar disks are cold enough to allow gas accretion near the central star. However, some astrophysical models (Schneider, 1996; Boss, 2002) predict that the formation of hot-Jupiters is unlikely to occur so close to central stars, thus proposing a postformation migration.

Interstellar dense molecular clouds represent another environment where phase Q noble gases could have been trapped.

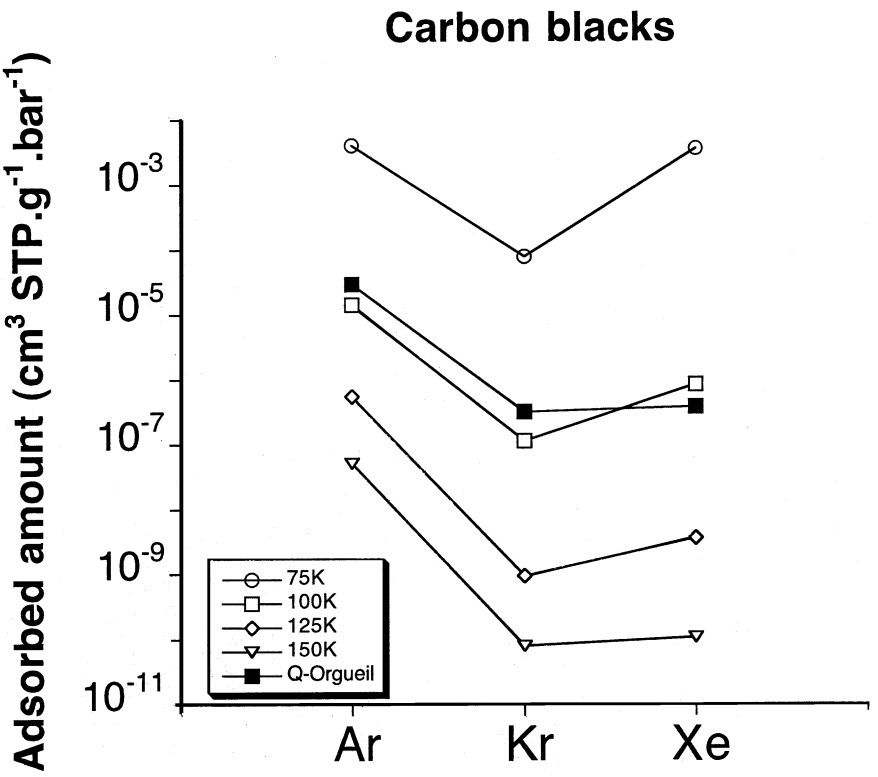

Fig. 9. (a) Elemental fractionation pattern for carbon blacks oxidized by HNO_3 at different temperatures.

With respect to this possibility, phase Q and nanodiamonds in primitives chondrites present a homogeneous distribution on a micron-scale (Huss and Alexander, 1987; Huss et al., 1996; Nakamura et al., 1999a,b; Amari et al., 2001, 2004). These authors have suggested that this distribution could be due to a presolar origin for phase Q and its trapped noble gases. Interstellar molecular clouds could have temperatures typically in the range 10 K–25 K. The lack of information concerning the noble gas partial pressure in the ISM as well as noble gas vapor pressures at very low temperature prevents us from quantitatively investigating noble gas adsorption on organic matter in the ISM. However, the present study documenting high noble gas adsorption at very low pressures and temperatures leaves open the possibility that Q noble gases originated in the ISM, as proposed by Sandford et al. (1998).

5. CONCLUSIONS

The present work provides results of an experiment designed to study adsorption of Ar, Kr, and Xe on materials found in primitive meteorites at pressures relevant to those inferred for the solar nebula. The adsorption efficiency increases from kerogen, carbon blacks, montmorillonite, to ferrihydrite. As most heavy noble gases in primitive meteorites are trapped in carbonaceous carriers, special attention was paid to kerogen and carbon blacks. Type III kerogen, which is a good chemical analog for phase Q (but not for its physical nature), has a low adsorption capacity. In contrast, carbon blacks, which are considered as potential precursors of phase Q (Vis et al., 2002), can adsorb high quantities of noble gases at low pressure. At 75 K, the noble gas amounts adsorbed on carbon black are up to two orders of magnitude higher than those found in phase Q. This work therefore shows that low-pressure physical adsorption of noble gases can account for the noble gas content observed in meteorites, even if only a few percent of adsorbed gases are irreversibly trapped. Irreversible adsorption could be facilitated by specific nebular conditions such as the occurrence of freshly created surfaces or radiation-induced defects (Bernatowicz et al., 1982; Hohenberg et al., 2002). As a consequence, it will be important to design low-pressure adsorption experiments in the presence of ionizing radiations.

Acknowledgments—Manuel Pelletier is thanked for assistance during sample analysis. We are grateful to Laurent Zimmermann and Pete Burnard for helpful discussions. Frédéric Villiéras is thanked for providing us with carbon black samples. We thank C. M. Hohenberg and two anonymous reviewers for constructive comments and Associate Editor R. Wieler for careful editing. This work was supported by the Programme National de Planétologie (Institut National des Sciences de l'Univers, CNRS). This is CRPG-CNRS contribution 1702.

Associate editor: R. Wieler

REFERENCES

Amari S., Zaizen S., and Matsuda J. (2001) Search for Q. *Meteorit. Planet. Sci.* **28,** A10–A11.

Amari S., Zaizen S., and Matsuda J. (2004) An attempt to separate Q from the Allende meteorite by physical methods. *Geochim. Cosmochim. Acta* **67,** 4665–4667.

Anders E. and Grevesse N. (1989) Abundances of the elements: Meteoritic and solar. *Geochim. Cosmochim. Acta* **53,** 197–214.

Anders E. and Zinner E. (1993) Interstellar grains in primitive meteorites: Diamond, silicon carbide and graphite. *Meteoritics* **28,** 490–514.

Bell K. R., Cassen P., Klahr H. H., and Henning T. (1997) The structure and appearance of protostellar accretion disks: Limits on disk flaring. *Astrophys. J.* **486,** 372–387.

Bell K. R. (1999) Reprocessing in luminous disks. *Astrophys. J.* **526,** 411–434.

Bell K. R., Cassen P., Wasson J. T. and Woolum D. S. (1999) The FU Orionis phenomenon and solar nebula material. In *Protostars and Planets IV* (eds. V. Manning, A. P. Boss and S. Russell), pp. 897–926. University of Arizona, Tuscon, AZ.

Bernatowicz T. J., Kramer F. E., Podosek F. A., and Honda M. (1982) Adsorption and excess fission Xe: Adsorption of Xe on vacuum crushed minerals. *J. Geophys. Res.* **87,** A465–A476.

Boss A. P. (1993) Evolution of the solar nebula. II. Thermal structure during nebula formation. *Astrophys. J.* **417,** 351–367.

Boss A. P. Stellar metallicity and the formation of extrasolar gas giant planets. *Astrophys. J.* **567** (*2*), L149–L153, 2002.

Brunauer S., Emmet P. H., and Teller E. (1938) Adsorption of gases in multimolecular layers. *J. Am. Chem. Soc.* **60,** 309–319.

Busemann H. and Eugster O. (2002) The trapped noble gas component in achondrites. *Meteorit. Planet. Sci.* **37,** 1865–1891.

Busemann H., Baur H., and Wieler R. (2000) Primordial noble gases in 'phase Q' in carbonaceous and ordinary chondrites studied by closed-system etching. *Meteorit. Planet. Sci.* **35,** 949–973.

Cameron A. G. W. (1995) The first ten million years in the solar nebula. *Meteoritics* **30,** 133–161.

Cassen P. (1994) Utilitarian models of the solar nebula. *Icarus* **112,** 405–429.

Collier Cameron A. (2002) Extrasolar planets: What are hot Jupiters made of? *Astro. Geoph.* **43** (**4),** 421–425.

Cornell R. M. and Schwertmann U. (1996) *The Iron Oxides.* VCH Verlag, Weinheim. 570 pp.

De Boer J. H., Lippens B. C., Linsen B. G., Brokhoff J. C. P., Van der Heuvel A., and Osinga T. J. (1966) The t-curve of multimolecular N_2 adsorption. *J. Colloid Interf. Sci.* **23,** 577–599.

Dubrulle B., Morfill G., and Sterzik M. (1995) The dust subdisk in the protoplanetary nebula. *Icarus* **114,** 237–246.

Dusham S. and Lafferty J. M. (1962) *Scientific Foundation of Vacuum Technique*, 2nd ed. Wiley. 806 pp.

Ehrenfreund P., Robert F., d'Hendecourt L., and Behar F. (1991) Comparison of interstellar and meteoritic organic matter at 3.4 μm. *Astron. Astrophys.* **252,** 712–717.

Fanale F. P. and Cannon W. A. (1972) Origin of planetary primordial rare gas: The possible role of adsorption. *Geochim. Cosmochim. Acta* **36,** 319–328.

Frick U. (1979) Noble gas fractionation during synthesis of carbonaceous matter. *Lunar and Planet. Sci X.* Lunar Planet. Inst., Houston (abstr.).

Gardinier A., Derenne S., Robert F., Behar F., Largeau C., and Maquet J. (2000) Solide state CP/MAS ^{13}C NMR of the insoluble organic matter of the Orgueil and Murchinson meteorites: Quantitative study. *Earth Planet. Sci. Lett.* **184,** 9–21.

Garrison D. H., Olinger C. T., Hohenberg C. M., and Caffee M. W. (1987) Noble gases in grain-size separates from Pesyanoe; a study in anomalous acquisition of terrestrial xenon. *Lunar and Planet. Sci. XIX.* Lunar Planet. Inst., Houston (abstr.).

Gregg S. J. and Sing K. S. W. (1982) *Adsorption, Surface Area and Porosity* 2nd ed Academic Press, London.

Hartmann L., Calvet N., Gulbring E., and D'Alessio P. (1998) Accretion and the evolution of T-Tauri disks. *Astrophys. J.* **495,** 385–400.

Hofmann A., Pelletier M., Michot L., Stradner A., Schurtenberger P., and Kretzschmar R. (2004) Characterization of the pores in hydrous ferric oxyde aggregates formed by freezing and thawing. *J. Colloid Interf. Sci.* **271,** 163–173.

Hohenberg C. M., Thonnard N., and Meshik A. (2002) Active capture and anomalous adsorption: New mechanisms for the incoporation of heavy noble gases. *Meteorit. Planet. Sci.* **37,** 257–267.

Humayun M. and Casssen P. (2000) Processes determining the volatile abundances of the meteorites and terrestrial planets. In *Origin of Earth and Moon* (eds. R. M. Canup and K. Righter), pp. 3–23. University of Arizona Press, Tuscon, AZ.

Huss G. R. and Alexander E. C. Jr. (1987) On the pre-solar origin of the normal planetary noble gas component in meteorites. *J. Geophys. Res.* **92**, (Suppl.) E710–E716.

Huss G. R., Lewis R. S., and Hemkin S. (1996) The "normal planetary" noble gas component in primitive chondrites: Compositions, carrier and metamorphic history. *Geochim. Cosmochim. Acta* **60,** 3311–3340.

Lewis R. S., Snivasan B., and Anders E. (1975) Host phase of a strange xenon component in Allende. *Science* **190,** 1251–1262.

Lewis R. S., Ming T., Wacker J. F., Anders E., and Steel E. (1987) Interstellar diamonds in meteorites. *Nature* **326,** 160–162.

Liang L. Y., Hofmann A., and Gu B. H. (2000) Ligand-induced dissolution and release of ferrihydrite colloids. *Geochim. Cosmochim. Acta* **64,** 2027–2037.

McClellan A. L. and Harnsberger H. F. (1967) Cross-sectional areas of molecules adsorbed on solid surface. *J. Colloid Interf. Sci.* **23,** 577–599.

Michot L., François M., and Case J. M. (1990) Surface heterogeneity studied by a quasi-equilibrium adsorption device. *Langmuir* **6,** 647–653.

Michot L. J., Villiéras F., Lambert J. F., Bergaoui L., Grillet Y., and Robert J. L. (1998) Surface heterogeneity of micropores in pillared clays: The limit of classical pore-filling mechanisms. *J. Phys. Chem. B* **102,** 3466–3476.

Michot L. J. and Villiéras F. (2002) Assessments of surface energetic heterogeneity of synthetic of Na saponite: The role of layer charge. *Clay Minerals* **37,** 39–57.

Nakamura T., Nagao K., Metzler K., and Takaoka N. (1999a) Heterogeneous distribution of solar and cosmogenic noble gases in CM chondrites and implications for the formation of CM parent bodies. *Geochim. Cosmochim. Acta* **63,** 257–273.

Nakamura T., Nagao K., and Takaoka N. (1999b) Microdistribution of primordial noble gases in CM chondrites determined by in situ laser microprobe analysis: Decipherment of nebular processes. *Geochim. Cosmochim. Acta* **63,** 241–255.

Nichols R. H. Jr., Nuth J. A. III, Hohenberg C. M., Olinger C. T., and Moore M. H. (1992) Trapping of noble gases in proton-irradiated silicates smokes. *Meteoritics* **27,** 555–559.

Niederman S. and Eugster O. (1992) Noble gases in lunar anorthositic rocks 60018 and 65315: Acquisition of terrestrial krypton and xenon indicating an irreversible adsorption. *Geochim. Cosmochim. Acta* **56,** 493–509.

Niemeyer S. and Marti K. (1981) Noble gas trapping by laboratory carbon condensates. *Proc. Lunar Planet. Sci.* **12B**, 1177–1188.

Nittler L. R. (2003) Presolar stardust in meteorites: Recent advances and scientific frontiers. *Earth Planet. Sci. Lett.* **6540,** 1–15.

Ott U., Mack R., and Chang S. (1981) Noble-gas-rich separates from the Allende meteorite. *Geochim. Cosmochim. Acta* **45,** 1751–1788.

Ozima M. and Podosek F. A. (2002) *Noble Gas Geochemistry.* Cambridge Univ. Press, Cambridge, U.K. 286 pp.

Ozima M., Wieler R., Marty B., and Podosek A. (1998) Comparative studies of solar, Q-gases and terrestrial noble gases and implications on the evolution of the solar nebula. *Geochim. Cosmochim. Acta* **62,** 301–314.

Pepin R. O. (1991) On the origin and early evolution of terrestrial planet atmospheres and meteoritic volatiles. *Icarus* **92,** 2–79.

Pepin R. O. (2003) On noble gas processing in the solar accretion disk, *Space Sci. Rev.* **106,** 211–230.

Podosek F. A., Bernatowicz T. J., and Kramer F. E. (1981) Adsorption of xenon and krypton on shales. *Geochim. Cosmochim. Acta* **45,** 2401–2415.

Podosek F. A. and Cassen P. (1994) Theoritical, observational and isotopic estimates of the lifetime of the solar nebula. *Meteoritics* **29,** 6–25.

Remusat L., Derenne S., and Robert F. (2003) Conventional and TMAH assisted pyrolysis on the insoluble organic matter of Orgueil and Murchison. *Lunar and Planet. Sci. XXXIV.* Lunar Planet. Inst., Houston. #1230 (abstr.).

Robert F. (2002) Water and organic D/H ratios in the solar system: A record of an early irradiation of the nebula? *Planet. Space Sci.* **50,** 1227–1234.

Sandford S. A., Bernstein M. P., and Swindle T. D. (1998) The trapping of noble gases by the irradiation and warming of interstellar analogs. *Meteorit. Planet. Sci.* **33,** A135.

Scherer P., Loeken T., and Schultz L. (1996) Changes in the noble gas pattern of hot desert meteorites caused by weathering: Correlation with terrestrial age and weathering grade. *Lunar and Planet. Sci. XXVII.* Lunar Planet. Inst., Houston. (abstr.).

Schneider D. (1996) Hot Jupiters. Why do some giant planets hug their stars? *Scientific American* **275** (*5*), 14–15.

Sosa R. C., Masy D., and Rouxhet P. G. (1993) Influence of surface properties of carbon black on the activity of adsorbed catalase. *Carbon* **32** (**7),** 1369–1375.

Sosa R. C., Parton R. F., Neys P. E., Lardinois O., Jacobs P. A., and Rouxhet P. G. (1996) Surface modification of carbon black by oxidation and its influence on the activity of immobilized catalase and iron-phthalocyanines. *J. Mol. Cata. A: Chemical* **110,** 141–151.

Srinivasan B., Lewis R. S., and Anders E. (1978) Noble gases in the Allende and Abee meteorites and a gas-rich mineral fraction: Investigation by stepwide heating. *Geochim. Cosmochim. Acta* **42,** 183–198.

Suzuki K. and Matsuda J.-I. (1990) Noble gases in the amorphous carbon synthesized by glow-discharge CVD. *Lunar and Planet. Sci. XXI.* Lunar Planet. Inst., Houston. (abstr.).

Takaishi M. and Sensui J. (1963) Corrections for thermal transpiration. *Tr. Farad. Soc.* **59,** 2503–2515.

Verchovsky A. B., Sephton M. A., Wrigth I. P., and Pillinger C. T. (2002) Separation of planetary noble gas carrier from bulk carbon in enstatite chondrites during stepped combustion. *Earth Planet. Sci. Lett.* **199,** 243–255.

Villiéras F., Cases J. M., François M., Michot L. J., and Thomas F. (1992) Texture and surface energetic heterogeneity of solids from modeling of low pressure gas adsorption isotherms. *Langmuir* **8,** 1789–1795.

Villiéras F., Michot L. J., Cases J. M., Berend I., Bardot F., François M., Gérard G. and Yvon J. (1996) Static and dynamic studies of the energetic surface heterogeneity of clay minerals. In *Equilibria and Dynamics of Gas Adsorption on Heterogeneous Solid Surfaces* (eds. W. Rudzinsky, W. A. Steele and G. Zgrablich), pp. 573–623. Elsevier Science Publisher B.V, Amsterdam.

Villiéras F., Michot L. J., Bardot F., Cases J. M., François M., and Rudzinsky W. (1997) An improved derivate isotherm summation method to study surface heterogeneity of clay minerals. *Langmuir* **13,** 1104–1117.

Villiéras F., Michot L. J., Bernaby E., Chamerois M., Legens C., Gérard G., and Cases J. M. (1999) High resolution gas adsorption study on mineral surfaces: Assessment of surface heterogeneity of calcite and apatite. *Colloids and Surfaces* **146,** 163–174.

Vis R. D., Mrowiec A., Kooyman P. J., Matsubara K., and Heymann D. (2002) Microscopic search for the carrier phase Q of the trapped planetary noble gases in Allende, Leoville and Vigarano. *Meteorit. Planet. Sci.* **37,** 1391–1399.

Wacker J. F. (1989) Laboratory simulation of meteoritic noble gases. III. Sorption of neon, argon, krypton and xenon on carbon: Elemental fractionation. *Geochim. Cosmochim. Acta* **53,** 1421–1433.

Wacker J. F., Zadnik M. G., and Anders E. (1985) Laboratory simulation of meteoritic noble gases. I. Sorption of xenon on carbon: Trapping experiments. *Geochim. Cosmochim. Acta* **49,** 1035–1048.

Wieler R., Anders E., Baur H., Lewis R. S., and Signer P. (1991) Noble gases in 'phase Q': Closed-system etching of an Allende residue. *Geochim. Cosmochim. Acta* **55,** 1709–1722.

Wieler R., Anders E., Baur H., Lewis R. S., and Signer P. (1992) Characterisation of Q-gases and other noble gas components in the Murchinson meteorite. *Geochim. Cosmochim. Acta* **56,** 2907–2921.

Wieler R. (2002) Noble gases in the solar system. *Rev. Mineral. Geochem.* **47,** 21–70.

Wood J. A. and Morfill G. E. (1988) A review of solar nebula models. In *Meteorites and the Early Solar System* (eds. J. F. Kerridge and M. S. Matthews), pp 329–347. University of Arizona Press, Tuscon, AZ.

Woolum D. S. and Cassen P. (1999) Astronomical constraints on nebular temperatures: Implications for planetesimal formation. *Meteorit. Planet. Sci.* **34** (*6*), 897–907.

Yang J., Lewis R. S., and Anders E. (1982) Sorption of noble gases by solids, with reference to meteorites. I. Magnetite and carbon. *Geochim. Cosmochim. Acta* **46,** 841–860.

Yang J. and Anders E. (1982a) Sorption of noble gases by solids, with reference to meteorites. II. Chromite and carbon. *Geochim. Cosmochim. Acta* **46,** 861–875.

Yang J. and Anders E. (1982b) Sorption of noble gases by solids, with reference to meteorites. III. Sulfides, spinels and other substances; on the origin of planetary gases. *Geochim. Cosmochim. Acta* **46,** 877–892.

Zadnik M. G., Wacker J. F., and Lewis R. S. (1985) Laboratory simulation of meteoritic noble gases. II. Sorption of xenon on carbon: Etching and heating experiments. *Geochim. Cosmochim. Acta* **49,** 1049–1059.

Zinner E. (1998) Stellar nucleosynthesis and the isotopic composition of presolar grains from primitive meteorites. *Ann. Rev. Earth Planet. Sci.* **26,** 147–188.

ELECTRONIC ANNEX

Supplementary data associated with this article can be found, in the online version, at doi:10.1016/j.gca.2004.09.016.